Environ Geol (2007) 52:1297–1306
DOI 10.1007/s00254-006-0568-7

ORIGINAL ARTICLE

The estimation of dispersion behavior in discrete fractured networks of andesite in Lan-Yu Island, Taiwan

Lee Cheng-Haw · Lee Chen-Chang · Lin Bih-Shan

Received: 13 September 2006 / Accepted: 23 October 2006 / Published online: 24 November 2006

Abstract This study was based on the discrete fracture model to investigate the influence of fracture parameters on the solute transport in the fractured rocks of andesite in Lan-Yu island, Taiwan. In the simulation cases, the centers of fractures, fracture lengths and apertures were assumed to have Poisson's distribution, negative exponential distribution and lognormal distribution, respectively. With the above assumptions, constructing the discrete fracture model became practicable. Using the mass-balance equation with specified boundary conditions, the flow field in the rock was solved. Then particles were released under the flow field. Monte Carlo method was used assuming that the amount of particles was proportional to the flow rates to get the particle accumulated percentage breakthrough curve and to estimate the dispersion coefficient. On the basis of the discrete fracture model, it was possible to evaluate the property of dispersion behavior of andesite in Lan-Yu Island with flow and transport mechanism. Properties of the dispersion behavior such as the relation between distance and traveling-time ($\ln\langle r^2\rangle$ and $\ln\langle t\rangle$), anisotropic behavior, and the overall dispersion coefficient in a fracture network were characterized: the slope value of $\ln\langle r^2\rangle$ and $\ln\langle t\rangle$ was 1.64 an indication of non-Fickian dispersion, the particles dispersion along the flow (D11) was bigger than that perpendicular to the flow (D22), and the dispersion coefficient by this study was 0.91 m comparing the value 1 m from Sauty's method.

Keywords Fracture networks · Particle tracking · Mote Carlo simulation · Dispersion behavior · Andesite

L. Cheng-Haw (✉) · L. Chen-Chang
Department of Resource Engineering,
National Chen Kung University,
Tainan, Taiwan, ROC
e-mail: leech@mail.ncku.edu.tw

L. Chen-Chang
Chemical Engineering, Institute of Nuclear Energy
Research Atomic Energy Council, Executive Yuan,
Taoyuan, Taiwan, ROC
e-mail: chenchang@iner.gov.tw

L. Bih-Shan
Department of Information Management,
Kao Yuan University, Kaohsiung, Taiwan, ROC

Nomenclature

b	Fracture aperture
L_f	Fracture length
μ_d	Dynamic viscosity of the fluid
Δh	Head difference
V_i	Velocity
x_i	Distances in the direction of flow
c	Solute concentration
D_{ij}	Dispersion coefficient tensor
g	Acceleration of gravity
Q_i	The ith flow rate
Q_{sum}	The total flow rate
x_0	Injection position
y_0	Injection position
θ	Fractal exponent
$\langle r^2\rangle$	Mean square travel paths displacement
$\langle t\rangle$	Particle travel time
BTC	Breakthrough curve of particles
BTC^a	Continuous breakthrough curve
BTC^p	Particle tracking breakthrough curve

S_t	Fracture spacing
W	The width of a square domain
w	Fracture width
x	Position of particle
y	Position of particle
α	Dispersivity
λ	Fracture frequency
ρ_f	Fracture density in a set
ρ	Density of the fluid
$\langle\rangle$	the average behavior

Introduction

A variety of modeling concepts has been proposed to characterize the transport of solutes in fractured media at the field scale. When classified according to how heterogeneity is incorporated in the model structure, fluid flow and solute transport fall into one of the three groups: discrete network models, equivalent continuum models, and hybrid models (National Research Council 2001). The development of elevated fluid pressures in permeable fractures having low shear strength and negligible tensile strength is a potential cause of rock deformation or failure in excavations and underground openings. This and the need to control seepage into mines and tunnels, and out of underground fluid storage caverns, render flow through permeable fractures of interest to mining and geotechnical engineers (Lee and Farmer 1993; Guguen and Boutca 2004; Newman 2005).

In many fractured rock studies, especially those concerning the safety of geologic nuclear waste repositories or other presently contaminated sites, a declared goal is to delineate existing or potential avenues of groundwater flow and solute migration (Neuman 2005). More recent theoretical and computational approaches in the discrete fracture networks are in the books of Sahimi (1995), Adler and Thovert (1999) and Zhang and Sanderson (2002). Most state of the art theoretical studies consider random networks of interconnected line segment in two dimensions (Clemo and Smith 1997; Lin and Lee 1998; Park et al. 2001a, b; Liu et al. 2002; Darcel et al. 2003; Ji et al. 2004; Bluma et al. 2005; Tran et al. 2006), or less commonly used in three-dimension (Margolin et al. 1998; Dershowitz and Fidelibus 1999; Park et al. 2002; Cvetkovic et al. 2004; Painter et al. 2006), embedded in an impermeable matrix. Each line segment is ascribed as a uniform transmissivity or width to which the transmissivity is related through a power (usually cubic) relationship (Newman 2005).

The international Stripa project has shown (S.K.B. 1993) that whereas it has been possible to construct both types of fracture network models for a large (125 m × 150 m × 50 m) undisturbed block of crystalline rock (the so-called site characterization and validation block) and to calibrate them against observed hydraulic and tracer data, these models have generally not performed better than much simpler and more parsimonious continuum or hybrid discrete models. So to use it or not is still an issue based on scale and cost (Newman 2005).

The objective of this study is to construct a 2D discrete fracture network model (Lin and Lee 1998), consisting of fracture density, length, aperture and orientation from the outcrop fracture data in Longman, Lan-Yu in Taiwan to evaluate the hydraulic properties of andesite. Particularly, dispersivity obtained from Sauty's solution (Sauty 1980) for a step function source in one-dimensional flow is estimated. This study showed that the engineer or researcher can get some initial idea of hydraulic properties in rock mass from the 2D discrete fracture network model.

Methods

The discrete fracture model was based on a statistical characterization of the rock mass. Generation of the fracture network was based not only on the assumption of the fracture parameter distributions (such as the fracture center, density and orientation), but also on the investigation of bedrock outcrops at the site. Here, the previous proposed method was used to generate the two-dimensional fracture network. The previous method focused on investigating the dispersion phenomenon and the power law relationship between mean square travel paths displacement $\langle r^2\rangle$ and particle travel time $\langle t\rangle$ based on percolation theory. This study puts emphasis on the match of the dispersivity of the flow field in a discrete fracture network.

Generation of 2D fracture networks

A two-dimensional bond percolation model was applied in this study in Fig. 1. This fracture network model was made through Poisson process (Clemo and Smith 1997) based on the assumption that the location and orientation of individual fractures are independent of all other fractures. The detailed processes of generating fractures could be also obtained from a previous study (Lee et al. 1993, 1994).

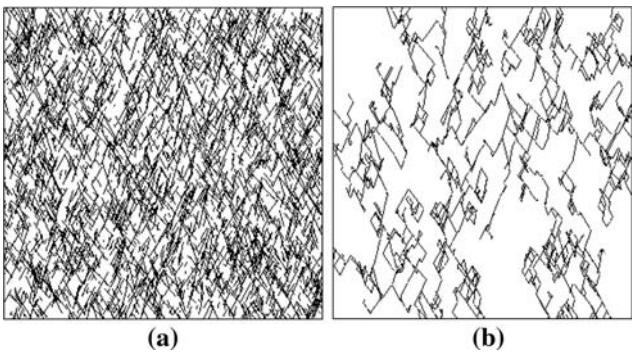

Fig. 1 **a** An original of the conductible network, and **b** the backbone of the fracture network in **a**

Flow theory

Flow rates going through the network were determined by the volumetric balance equations for each node, considering that the algebraic sum of the fluxes at each node was equal to zero. The Hagen-Poiseuille law was invoked for the flow rate calculation through a fracture given by

$$Q = b^3 \rho w g \Delta h / (12 \mu_d L_f) \quad (1)$$

b is the fracture aperture, w is fracture width, ρ is the density of the fluid, g_f is the acceleration of gravity, L_f is the fracture length, μ_d is the dynamic viscosity of the fluid, and Δh is the head difference between the inlet and outlet of the fracture. A volumetric balance equation at each node was applied to a set of linear algebraic equations. This system was solved under the assumed boundary conditions (Fig. 2), providing pressure at each node in the network. Then, with the quantification of fracture apertures, the flow rate and fluid velocity were solved in the two nodes of a fracture. Therefore, with the above procedure, the flow field could be determined in the fracture network.

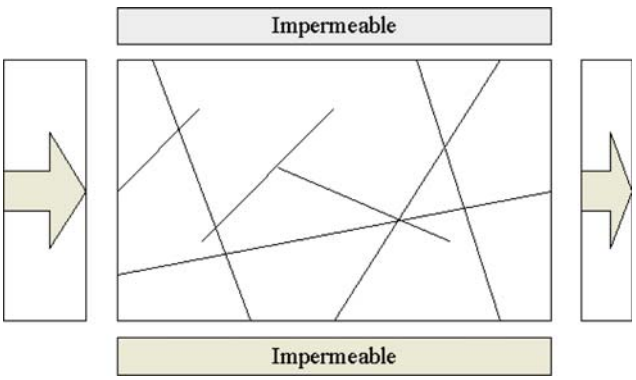

Fig. 2 The conceptual model of the domain showing that upper and lower bound are no flow boundary and the arrow means the flow direction by the gradient 0.01

Particles' transport theory

Within the flow field proposed above, it was assumed that the particles movement can be described by

$$\frac{\partial c}{\partial t} = -V_i \frac{\partial c}{\partial x_i} + \frac{\partial}{\partial x_i}\left(D_{ij} \frac{\partial c}{\partial x_i}\right) \quad (2)$$

V_i is the velocity, x_i is the distances in the direction of flow, c is the solute concentration and D_{ij} is the dispersion coefficient tensor. Equation 2 entailed a numerical approximation (Bear 1972) given as:

$$\frac{c}{c_0} = \frac{1}{2}\left\{1 \pm \mathrm{erf}\left(\frac{x - vt}{\sqrt{4Dt}}\right)\right\} \mathrm{if}^{x-vt<0+}_{x-vt>0-} \quad (3)$$

c_0 was initial concentration. For flow in a single fracture, the particles' transport could be regarded as one dimensional transport so that

$$D = \alpha V \quad (4)$$

where D was the dispersion coefficient, α was the dispersivity and V was the average velocity.

Particle tracking

In the discrete fracture model, the transport simulation was based on a Monte Carlo particle tracking algorithm. The Monte Carlo process was based on both the direction of flow and discharge in the fractures. When a particle left a fracture and entered a node, the adjoining fractures were examined to recognize whether or not their flow direction was away from the node. The particle then moved into one of these fractures in which the probability of entry into each fracture was proportional to its flow rate. Repeating the procedure enabled the motion of a large number of particles to be tracked, approximating the movement of solute, throughout the modeling domain. Computer simulations of the random walk were performed with 1,000 particles tracked through the system in each case (Lin and Lee 1998). Particles moved in discrete steps from node to node with the time taken to move being the bulk fluid velocity divided by distances between nodes. Solute diffusion was assumed to be large enough to mask the effect of the velocity profile that develops in laminar flow within fractures. Longitudinal diffusion within fractures segments was considered to be negligible. At fracture intersections, the fluid was

assumed to mix completely leading to a stochastic transport algorithm. Particles entered fractures randomly from a fracture intersection. The probabilities of entering fractures are consistent with the flow entering the fracture.

Dispersivity estimation

From Eq. 3 a continuous breakthrough curve, BTC^a could be drawn. This breakthrough curve is analogous to the discrete breakthrough curve, BTC^P, made from the Monte Carlo simulation. In this study, the superscript "*a*" denotes the "analytical breakthrough curve" and superscript "*p*" denotes the "particle tracking breakthrough curve". The dispersion coefficient D of BTC^a was estimated from BTC^P. The algorithm to calculate dispersivity is shown in Fig. 3. Because the dispersivity estimated by this algorithm was a bulk dispersivity, the type of particle injection was "all inlets injection". The algorithm is described below:

1. Assuming there were *m* openings over the high head side. Same amount of particles were injected into individual *i*th opening to obtain an individual BTC_i^P. Meanwhile, the BTC_i^P the flow rate Q_i of the *i*th opening was obtained from the flow field. The average velocity was

$$V_i = W/t_{50i} \tag{5}$$

where V_i the average velocity, W was the width of a square domain and t_{50i} the average time of a particle cross the domain. In addition, the maximum and minimum breakthrough time ($T_{\max}$ and $T_{\min}$) among all particle tracking breakthrough curves (BTC_i^P) were also obtained. The total flow rate Q_{sum} was calculated by

$$Q_{\text{sum}} = \sum_{i=1}^{m} Q_i \tag{6}$$

2. Because the particles intermittently reached the low head boundary for a BTC_i^P, there were several time-points when particles arrived indicating that the time-varying arrival particles would change at the time point of the low head boundary. The concentration ratio, of BTC_i^P for ith injection point at *k*th time-point t_k was denoted, $(c/c_0)^P_{k,i}$. In another hand, taking $x = W$ and $v = V_i$ $t = t_k$ and an arbitrarily D value into Eq. 3, an approximate $(c/c_0)^a_{k,i}$ was also found. A D_i was estimated when $[(c/c_0)^P_{k,i} - (c/c_0)^a_{k,i}]^2$ approached a minimum. This procedure transformed BTC_i^P from discrete pattern into an analog continuous pattern, so that

$$\text{BTC}_i^P \approx \text{BTC}_i^{a^*} \tag{7}$$

the asterisk mark indicated the analytical breakthrough curve was transformed from BTC_i^P.

3. Dividing $T_{\min}$ and $T_{\max}$ into N time steps and the *j*th time step called T_j. $BTC_i^{a^*}$ was having a corresponding $(c/c_0)_j$ from Eq. 3 at each time step. Thus, the global approximate breakthrough curve, $BTC_G^{a^*}$, was expressed as:

$$\text{BTC}_G^{a^*} \approx \frac{1}{Q_{\text{sum}}} \sum_{i=1}^{m} Q_i (c/c_0)_j, \quad j = 1, N \tag{8}$$

$$\text{BTC}_G^{a^*} \approx (c/c_0)_j^G, \quad j = 1, N \tag{9}$$

Eqs. 8 and 9 integrated BTC_i^P into $BTC_G^{a^*}$ The approximate mark was used because BTC_G^a was interpreted from the individual $(c/c_0)_j$ and was not strictly equivalent to the sum.

4. The t_{50G} of BTC_G^a was interpolated by T_j and T_{j+1} that were close to 50% breakthrough of $(C/C_0)^G$. Again let $x = W$, $t = T_j$. By systematically

```
for each i injection opening
{
Calculate Q_i
Lead in BTC_i^P obtained from particle tracking method.
Obtain t50_i and Calculate V_i
    for each k reach time-point
    {
        {for each D from a little test value to a large big test value step increment
            {
                sumation [(C/C0)^P_{k,i} - (C/C0)^a_{k,i}]
            }
            if sumation [(C/C0)^P_{k,i} - (C/C0)^a_{k,i}] is minimum then save D as D_i
        }
    }
    save the minimum breakthrough time T_min
    save the maximum breakthrough time T_max
    sumation Q_i
}
for each i injection opening
{
    for each j time step starts from T_min to T_max
        {
            {for each D from a little test value to a large big test value step increment
            {
                sumation [(C/C0)^G_j - (C/C0)^a_j]^2
            }
            if sumation [(C/C0)^G_j - (C/C0)^a_j]^2 is minimum then save D as D_G
        }
}
interpolate t50G from (C/C0)^G_j
calculate V_G
dispersion coefficient= D_G/V_G
```

Fig. 3 The algorithm to obtain dispersion coefficient

introducing different values of D, an approximate $(c/c_0)_j^a$ at jth time step was found. A D_G was estimated when $[(c/c_0)_j^G - (c/c_0)_j^a]^2$ approaches a minimum. Take global average time (t_{50G}) into Eq. 5 obtain an average velocity

$$V_G = W/t_{50_G} \tag{10}$$

Introducing D_G as D and Eq. 10 into Eq. 4, the global dispersion coefficient of the sample region was obtained. The above procedure in Figs. 3 and 4 were mainly for the purpose of getting the value of dispersion coefficient D. In Fig. 5, the solid line was the particle tracking method and the dot line was the matching curve method proposed above and this graph showed that the curves compare quite well with each other.

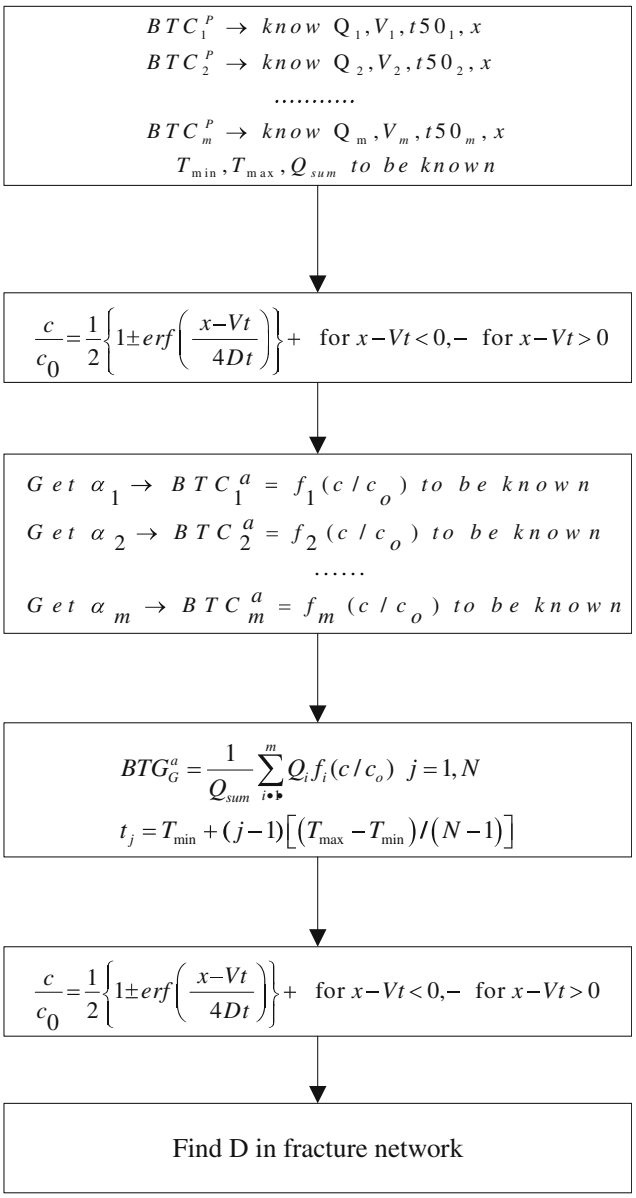

Fig. 4 Using the BTC^P and BTC^a to get the overall dispersion coefficient

Dispersion tensor estimation

It is noteworthy that when investigating the anisotropic dispersion, the particles injection was performed at the high-head side inlet which possessed a relative maximum flow rate. This location must be away from the no-flow boundaries. Two reasons for this choice were: (1) the extremely uneven flow leading to a concentration of the flow along preferred flow paths (Nordqvist et al. 1992) so that the particles were assumed to travel in the preferential path, i.e., the path of maximum flow rate, and (2) to characterize the dispersion without the influence of other injections (Lin and Lee 1998).

Berkowitz and Breaster (1991) proposed a fractal concept to describe the particle movement:

$$\langle r^2 \rangle \sim t^{\theta} \tag{11}$$

where

$$r^2 = (x - x_0)^2 + (y - y_0)^2 \tag{12}$$

x and y were the position of particle and x_0 and y_0 were the injection position. $\langle r^2 \rangle$ was the average r^2 of a particle population. θ was a fractal exponent, or the slope of log–log crossplot of Eq. 11. Their work depicted only the fractal dimension. So, the anisotropy of dispersion could also be characterized by Schwartz and Smith (1988) and Way and McKee (1981) who proposed a generalized theory of an isotropic dispersion in two-dimension fracture networks. This work is quite important because it provided a complete picture of anisotropy in fracture networks. And the dispersion tensor could be given as:

$$D_{ij} = \begin{bmatrix} D_{xx} & D_{xy} \\ D_{yx} & D_{yy} \end{bmatrix} \tag{13}$$

$$D_{xx} = \frac{\left(\langle xx \rangle - 2\langle xt \rangle \langle x \rangle / \langle t \rangle + \langle tt \rangle \langle x \rangle^2 / \langle t \rangle^2\right)}{2\langle t \rangle} \tag{14}$$

$$D_{xy} = D_{yx} = \frac{\left(\langle xy \rangle - \frac{\langle xt \rangle \langle y \rangle}{\langle t \rangle} - \frac{\langle yt \rangle \langle x \rangle}{\langle t \rangle} + \frac{\langle tt \rangle \langle x \rangle \langle y \rangle}{\langle t \rangle^2}\right)}{2\langle t \rangle} \tag{15}$$

$$D_{yy} = \frac{\left(\langle yy \rangle - \frac{2\langle yt \rangle \langle y \rangle}{\langle t \rangle} + \frac{\langle tt \rangle \langle y \rangle^2}{\langle t \rangle^2}\right)}{(2\langle t \rangle)} \tag{16}$$

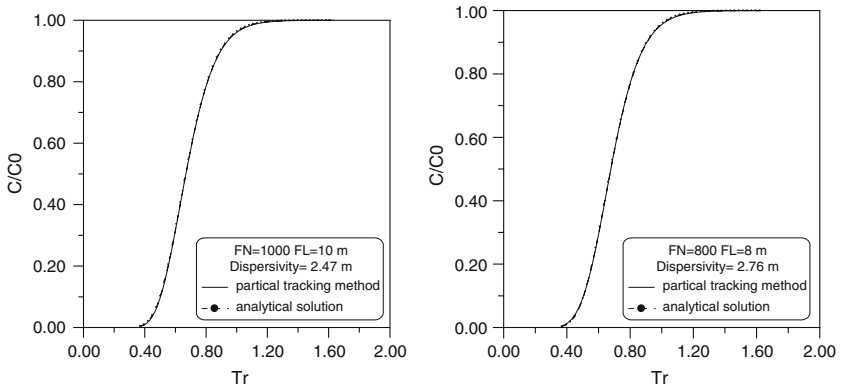

Fig. 5 Two realizations of matching procedure (Tr = $V \times T/L$; *FN* fracture number; *FL* fracture length)

where D_{ij} was dispersion tensor, D_{xx} was dispersion tensor component in x direction, D_{xy} was dispersion tensor component between x and y direction, and D_{yy} was dispersion tensor component in y direction; $\langle\rangle$ was the average behavior, t was the residence time of a particle swarm after transport through an portion of the network; x was the displacement with coordinates x, y was the displacement with coordinates y; xx, xy, yy, xt, yt, and tt were the product of x square, x and y, y square, x and t, y and t, and t square.

The calculations of anisotropic dispersion are valid only until the first particle leaves the network namely, the first particle reached the downstream boundary. Once D_{xx} D_{xy} D_{yy} had been calculated, the major and minor dispersion tensor could be expressed as (Way and Makee 1981).

$$D_{11} = \frac{(D_{xx} + D_{yy})}{2} + \frac{[(D_{xx} - D_{yy})^2 + 4D_{xy}^2]^{0.5}}{2} \quad (17)$$

$$D_{22} = \frac{(D_{xx} + D_{yy})}{2} - \frac{[(D_{xx} - D_{yy})^2 + 4D_{xy}^2]^{0.5}}{2} \quad (18)$$

where D_{11} was the major principal dispersion coefficient and D_{22} was the minor principal dispersion coefficient.

Thus, the 2D dispersion tensors and anisotropic ratio, defined as D_{11}/D_{11}, could be calculated from the stochastic description of particle spreading, and, these would promote more understanding of particles' transport.

Site description

The study area, Lan-Yu island, was about 49 miles southeast of Taitung city in the southeast part of Taiwan and encompassed an area of about 45.79 km^2. The study site in the southeast part of Lan-Yu Island (Fig. 6) is freshly fractured andesite. Investigations of the fracture geometric parameters such as the fracture sets, the mean orientation, the frequency, the spacing and the trace length were conducted on the field outcrop (Table 1; Fig. 7, see also Chen et al. 2001). The focus in this site was not only on the surface outcrop of

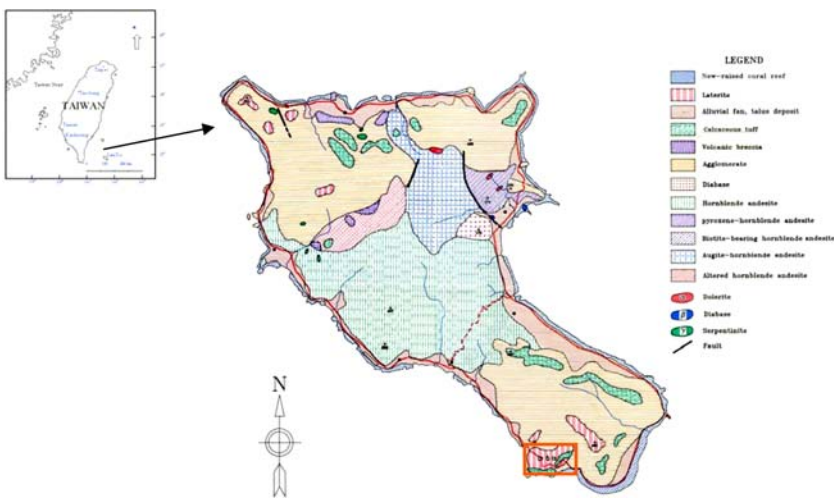

Fig. 6 Location of Lan-Yu LLW site and its geologic map

Table 1 The mean orientation and spacing of fractured rocks in Lan-Yu site. (Chen et al. 2001)

Set	Trend (°)	Plunge (°)	Frequency (fractures/m)	Mean spacing (m)
1	41.3	16.6	1.44	0.69
2	311.2	29.6	0.68	1.50
3	133.9	20.3	0.75	1.33
4	213.2	19.6	2.63	0.38

fractures but also the hydrogeology investigation from the previous study (Lee et al. 1996) showing that the transmissivity was estimated with a value of 8.9×10^{-4} m/s and the Field double-ring test was also applied here indicating that the surface hydraulic aperture was 0.191 mm. The upper transmissivity bound from the double-ring test was 3.81×10^{-4} m/s, the lower bound was 2.27×10^{-5} m/s, and the average hydraulic conductivity was 8.04×10^{-4} m/s. Therefore, from the below equation (Chen et al. 2001)

$$k_f = \frac{\boldsymbol{\rho} g b_h^2}{12\boldsymbol{\mu}_{\mathrm{d}}} \tag{19}$$

the upper bound of aperture was 0.41 mm, the lower bound was 0.032 mm and the difference between the upper and lower was 0.182 mm used for the standard deviation and assumed the aperture was lognormal distribution.

From the Table 1 and the Fig. 7 the first and the fourth set, the second and the third set were quite close to each other, so the four sets were combined to make the main two sets. The new first set had 72 fractures and trace angle and average fracture length were 68.3° and 0.348 m individually, and the second set had 56 fractures and trace angle and fracture length were 119.2° and 0.399 m individually. For the sampling area boundary limit, the estimates of fracture lengths which maybe truncated at the sampling outline and its distribution is always difficult to evaluate. So, the fracture length distribution in our study is using by the intersection of planar rock face of the distribution of trace lengths (Priest and Hudson 1981) as our fracture length distribution. The modeling domain should be larger than the representative volume (REV), so from the equation (Priest 1993):

$$W_{\mathrm{REV}} = B_{\mathrm{REV}} = (10 \sim 50) S_t \tag{20}$$

$$\lambda = 1/S_t = 2\rho_{\mathrm{f}} L/\pi \tag{21}$$

where S_t was the fracture spacing, λ was the fracture frequency, ρ_{f} was fracture density in a set, and L was the fracture average length.

The estimation of the REV was 30 times the fracture spacing, so from Eq. 20 the first set REV was estimated as 7.5 m and second set was estimated as 8.4 m. For the convenience in modeling, the domain in 2D fracture network was assumed to be 10 m × 10 m and the input parameter values were those shown in Table 2. The fracture parameter distribution, the centers of fractures, fracture lengths and apertures were assumed to be a Poisson distribution, negative exponential distribution and lognormal distribution, respectively. Under the above assumptions, constructing the discrete fracture model became practicable (Fig. 8).

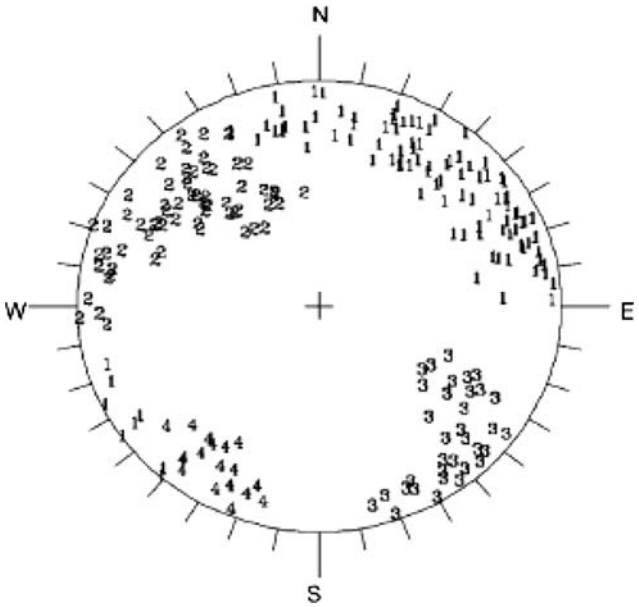

Fig. 7 Pole diagram of fracture orientation at the Lan-Yu site on a Schmidt net. The *number* indicates the set number

Results and discussion

The dispersion behavior of particle transport in fracture networks was an important problem to discuss and this study proposed the preliminary research on the dispersion, and anisotropic transport behavior of particles using the discrete fracture model. On the part of

Table 2 Input parameter considered in this study

Set	FN	FL (m)	FA (°)	FAD (°)	Aperture (mm)	Domain size
1	1800	0.348	68.3	15	mean 0.191	10 m × 10 m
2	1300	0.399	119.2	15	std 0.182	

FN fracture numbers, *FL* fracture length, *FA* fracture angle, *FAD* fracture angle deviation

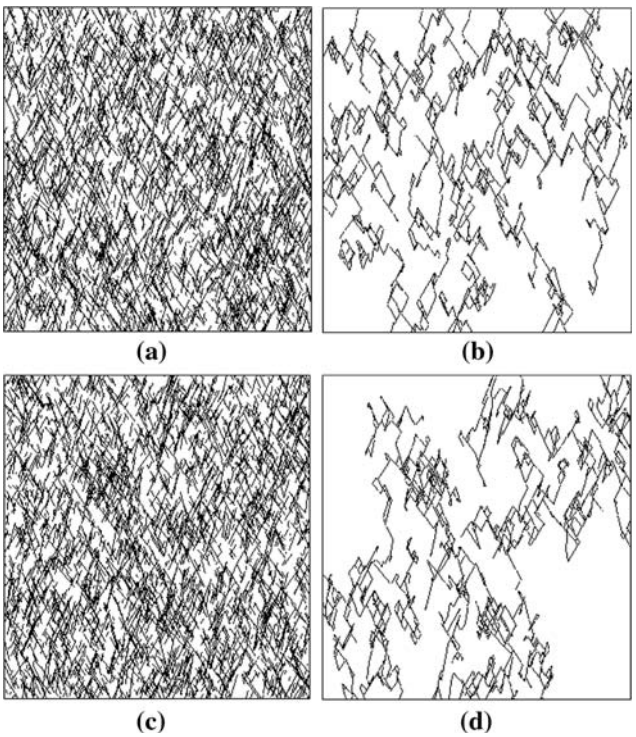

Fig. 8 Two realization of the fracture network population in Longman area (**a**), **c** an original of fracture network in Longman and (**b**, **d**) the backbone of the fracture network

the dispersion match, Fig. 9a represents the type curve of various values of Peclet number and Fig. 9b shows the matching using the proposed method and the Sauty's method from the concept of Peclet number. The solid line was from Sauty's method and the dotted line was from this study. This match between the curves was quite close and the error was about 0.09% and it was estimated by the mean error between the solid and dotted line.

The dispersion was characterized by a coefficient in the macroscopic transport equation (i.e. characterizing the processes at scales larger than the heterogeneity). As the Eq. 2 where C was the macroscopic concentration of the conservative solute, V was the macroscopic fluid velocity and D the effective macroscopic dispersion coefficient expected to increase with scale due to velocity heterogeneities similarly to what has been described by (Gelhar and Axness 1983) in porous media. This dispersion match had something quite different from the non-Fickian study (Kosakowski et al. 2001) for in Fig. 3 at the first matching step some error occurring in the beginning and the ending part of the discrete breakthrough curve for each particle movement(fractal-like behavior) is still existing but at the second matching step the breakthrough curve of each particle movement will eliminate the error of that, so it will become smoother than the first one, even though the discrete particle movement is fractal like at the first step. So, finally the overall of the breakthrough curve will be compared with Sauty (1980) and the Peclect number matched was ten in one realization.

The anisotropic transport behavior of particles was shown in Fig. 10a the relationship between $\ln\langle r^2\rangle$ and $\ln\langle t\rangle$ was linear and to investigate the dispersion coefficient in fracture networks, this should be discussed first on the validating the form $\langle r^2\rangle \sim t^d$ (r: the travel distance of particles in fracture networks, t: the travel time of particles in fracture networks). The finding suggests that the form $\langle r^2\rangle \sim t^d$ was valid in the fractured networks for describing the dispersion of particle transport. Comparing $\langle r^2\rangle$ and a certain t revealed that the speed of particle transport increased as the fracture length was extended. In Fig. 10a the slope values ranged from 1.29 to 1.65 and in Fig. 10b the slope value was 1.64, indicating that the behavior was not Fickian. Dispersion is considered fractal for a slope bigger than 1.27 (Sahimi and Imdakm 1988; Lin and Lee 1998).

Figure 11 shows that anisotropic dispersion also occurred in the fractured networks. In the simulation case, the flow direction of D_{11} (parallel to the mean flow direction) was quite bigger than D_{22} (perpendicular to the mean flow direction), indicating that the particles in the parallel to the mean flow direction may spread faster than the perpendicular to the mean flow

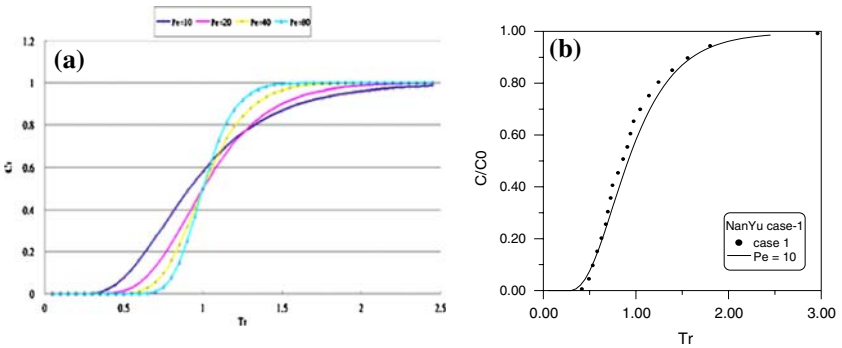

Fig. 9 **a** The match curve from the Sauty's solution at different Peclet number. **b** One match realization of the population in Longman area. (Tr = VT/L)

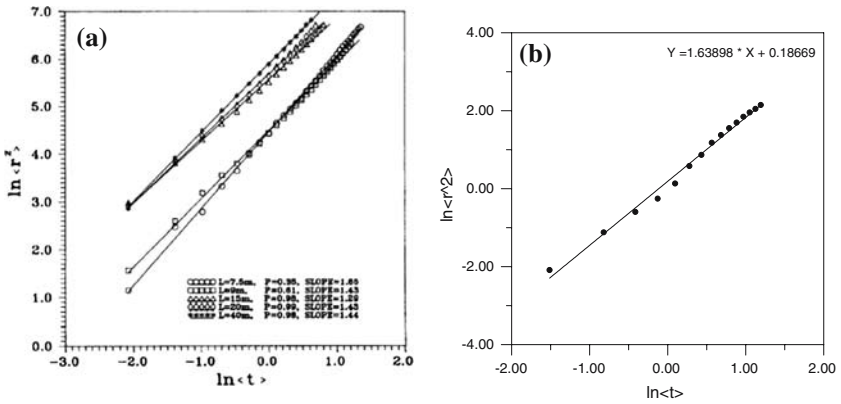

Fig. 10 **a** Fitting of ln $\langle r^2 \rangle$ versus ln$\langle t \rangle$ for mean fracture length L (Lin and Lee 1998). **b** This study in Longman area

direction, therefore the movement of particles will not be similar to that in porous media and as mentioned above it will exhibit fractal behavior in the discrete breakthrough curve.

Conclusion

This study provided a general method of analyzing the dispersion phenomenon through a fracture network, especially in the estimation of dispersion coefficient without detailed information on the geometrical and hydraulic characteristics. The proposed matching procedure also provides a means to determine the dispersion coefficient in fractured networks, and the anisotropic tensor and the fractal relation of ln$\langle r^2 \rangle$ and ln$\langle t \rangle$ were used to demonstrate the particles' behavior in fractured networks.

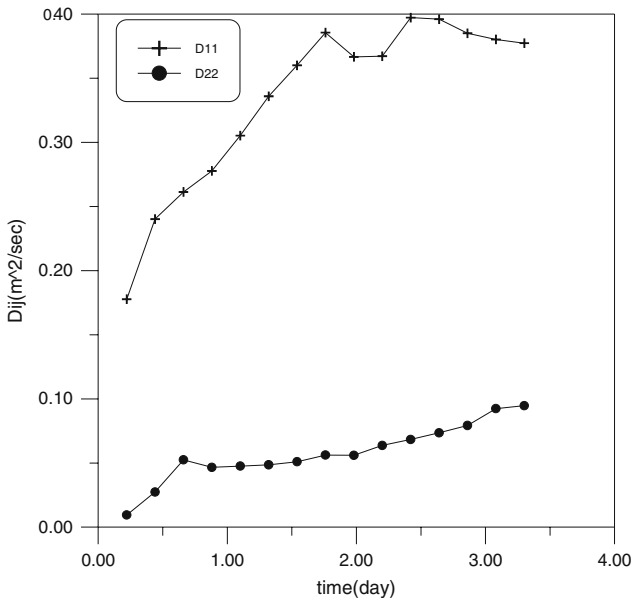

Fig. 11 The relationship between the time and the dispersivity for D_{11} and D_{22}

This study developed an approach to investigate the dispersion coefficient and the evaluation of dispersion behavior of particles in fracture networks. The results indicated that a linear relationship between ln$\langle r^2 \rangle$ and ln$\langle t \rangle$ in Longman area in Lan-Yu island of Taiwan was 1.64 showing that the dispersion in a fracture network was considering to be not purly diffusion for particles would travel in the flow-driven fracture, and therefore Fickian dispersion would not appear as the behavior as the porous media would.

Based on the isotropic tensor estimation of dispersion, it showed that the particles' movement would be along the direction of the hydraulic gradient vector. That also indicated that the fracture flow would be the most important factor to consider in the fracture networks. Under the hypothetical boundary condition simulating particles behavior in the Longman area, it showed that the error between the proposed dispersion coefficient and Sauty's method was about 0.09% indicating that this proposed method would be reasonable. This study has proposed a method to evaluate the particles transport in fracture network at the Longman low level radioactive disposal site in Lan-Yu island of Taiwan using surface fracture survey data. This was a preliminary study of this site, and it was proposed that scale effect should be taken into consideration.

Acknowledgments The authors would like to express their gratitude to the National Science Council of R.O.C. and Taiwan Power Company for the financial support under the grant number NSC-89-TPC-7-006-013. Comments from Tom Clemo in CGISS of Boise State University, Bill Arnold in Sandia Nation Laboratory and one anonymous reviewer are appreciated.

References

Adler PM, Thovert JF (1999) Fractures and fracture networks, theories and applications of transport in porous media, vol 15, Kluwer, Dordrecht, pp 429

Bear J (1972) Dynamics of fluids in porous media. Elsevier, New York

Berkowitz B, Breaster C (1991) Dispersion in sub-representative elementary volume fracture networks: percolation theory and random walk approaches. Water Resour Res 27(2):3159–3164

Bluma P, Mackaya R, Rileya MS, Knight JL (2005) Performance assessment of a nuclear waste repository: upscaling coupled hydro-mechanical properties for far-field transport analysis. Int J Rock Mec Min Sci 42:781–792

Chen RH, Lee CH, Chen CS (2001) Evaluation of transport of radioactive contaminant in fracture rock. Environ Geol 41:440–450

Clemo TM, Smith L (1997) A hierarchical model for solute transport in fracture media. Water Resour Res 33(7):1763–1783

Cvetkovic V, Painter S, Outters N, Selroos JO (2004) Stochastic simulation of radionuclide migration in discretely fractured rock near the Aspo Hard Rock Laboratory. Water Resour Res 40(1):1502–1513

Darcel C, Bour O, Davy P, De Dreuzy JR (2003) Connectivity properties of two-dimensional fracture networks with stochastic fractal correlation. Water Resour Res 39(10):1272–1285

Dershowitz WS, Fidelibus C (1999) Derivation of equivalent pipe network analogues for three-dimensional discrete fracture networks by the boundary element method. Water Resour Res 35(9):2685–2691

Gelhar LW, Axness CL (1983) Three-dimensional stochastic analysis of macrodispersion. Water Resour Res 19(1):161–180

Guguen Y, Boutca M (2004) Mechanics of fluid saturated rocks. Academic, New York, pp 416

Ji SH Lee KK, Park YC (2004) Effects of the correlation length on the hydraulic parameters of a fracture network. Transp Porous Media 55:153–168

Kosakowski G, Berkowitz B, Scher H (2001) Analysis of field observation of tracer transport in a fractured till. J Contam Hydrol 47:29–51

Lee CH, Farmer I (1993) Fluid flow in discontinuous rock. Chapman & Hall, London, pp 169

Lee CH, Yu JL, Hwung HH (1993) Fluid flow and connectivity in fractured rock. Water Resour Manage 7:169–184

Lee CH, Lin BS, Yu JL (1994) Dispersion and connectivity in flow through fractured network. J Chin Inst Eng 17(4):521–535

Lee CH, Chang JL, Hsu KT (1996) Investigation of hydraulic aperture at surface-exposed rock fractures in stiu. Geotechnique 46:343–349

Lin BS, Lee CH (1998) Percolation and dispersion of mass transport in saturated fracture networks. Water Resour Manage 12:409–432

Liu HH, Bodvarsson GS, Finsterle S (2002) A note on unsaturated flow in two-dimensional fracture networks. Water Resour Res 38(9):1176–1191

Margolin G, Berkowitz B, Scher H (1998) Structure flow and generalized conductivity scaling in fracture networks. Water Resour Res 34(9):2103–2121

National Research Council (2001) Conceptual models of flow and transport in the fractured vadose zone. National Academy, Washington, p 374

Neuman SP (2005) Trends, prospects and challenges in quantifying flow and transport through fracture rocks. Hydrogeol J 13:124–147

Nordqvist AW, Tsang YW, Tsang CF, Dverstorp B, Anderson J (1992) A variable aperture fracture network model for flow and transport in fractured rocks. Water Resour Res 28(6):1703–1713

Park BY, Kim KS, Kwon S, Kim C, Bae DS, Hartley LJ, Lee HK (2002) Determination of the hydraulic conductivity components using a three-dimensional fracture network model in volcanic rock. Eng Geol 66:121–174

Park YJ, Lee KK, Berkowitz B (2001a) Effects of junction transfer characteristics on transport in fracture networks. Water Resour Res 37(4):909–923

Park YJ, De Dreuzy JR, Lee KK, Berkowitz B (2001b) Transport and intersection mixing in random fracture networks with power law length distributions. Water Resour Res 37(10):2493–2501

Painter Scott L, Vladimir Cvetkovic, Osvaldo Pensado (2006) Time domain random walk algorithms for simulating radionuclide transport in fractured porous rock, IHLRWM, Las Vegas, April30–May 4, pp 293–300

Priest SD (1993) Discontinuity analysis and for rock, Engineering. Chapman & Hall, London

Priest SD, Hudson JA (1981) Estimation of discontinuity space and trace length using scanline survey. Int J Rock Mech Min Sci Geomech Abstr 18:183–197

Sahimi M (1995) Flow and transport in porous media and fractured rock: from classical methods to modern approaches. Wiley, New York, pp 483

Sahimi M, Imdakm AO (1988) The effect of morphological disorder on hydrodynamic dispersion in flow through porous media. J Phys A Math Gen 21:3833–3870

Sauty JP (1980) An analysis of hydrodispersive transfer in aquifer. Water Resour Res 16(1):145–148

Schwartz FW, Smith L (1988) A continuum Approach for Modeling Mass Transport in Fractured Media. Water Resour Res 19(4):959–969

S.K.B. Swedish Nuclear Fuel and Waste Management Co. (1993) SKB annual report 1992, SKB Stripa Project Technical Report TR 92–46, Stockholm

Tran Nam H, Chen Zhixi, Rahman Sheik S (2006) Integrated conditional global optimisation for discrete fracture network modeling. Comput Geosci 32:17–27

Way SC, McKee CR (1981) Restoration and In-Stiu coal gasfication sites from naturally occurring flow and dispersion. In-stiu Consult Inc 5(2):77–101

Zhang X, Sanderson DJ (2002) Numerical modeling and analysis of fluid flow and deformation of fractured rock masses. Elsevier, Amsterdam, p 300